Synchronization and Phase Noise Reduction in Micromechanical Oscillator Arrays Coupled through Light

Mian Zhang,[1] Shreyas Shah,[1] Jaime Cardenas,[1] and Michal Lipson[1,2,*]
[1]School of Electrical and Computer Engineering, Cornell University, Ithaca, New York 14853, USA
[2]Kavli Institute at Cornell for Nanoscale Science, Ithaca, New York 14853, USA
(Received 19 May 2015; published 16 October 2015)

Synchronization of many coupled oscillators is widely found in nature and has the potential to revolutionize timing technologies. Here, we demonstrate synchronization in arrays of silicon nitride micromechanical oscillators coupled in an all-to-all configuration purely through an optical radiation field. We show that the phase noise of the synchronized oscillators can be improved by almost 10 dB below the phase noise limit for each individual oscillator. These results open a practical route towards synchronized oscillator networks.

DOI: 10.1103/PhysRevLett.115.163902 PACS numbers: 42.82.Et, 05.45.Xt, 07.10.Cm, 85.85.+j

Nano- and micromechanical oscillator arrays have the potential to enable high power and low noise integrated frequency sources that play a key role in sensing and the essential time keeping of modern technology [1–5]. The challenge with building scalable oscillator arrays is that micromechanical oscillators fabricated on a chip fundamentally have a spread of mechanical frequencies due to unavoidable statistical variations in the fabrication process [4,6–9]. This dispersion in mechanical frequencies has a detrimental effect on the coherent operation in arrays of micromechanical oscillators. Here, we show that arrays consisting of three, four, and seven dissimilar microscale optomechanical oscillators can be synchronized to oscillate in unison, coupled purely through a common optical cavity field using less than a milliwatt of optical power. We further demonstrate that the phase noise of the oscillation signal can be reduced by a factor of N below the thermomechanical phase noise limit of each individual oscillator as N oscillators are synchronized, in agreement with theoretical predictions [10,11]. The highly efficient, low loss, and controllable nature of light mediated coupling could put large scale nano- and micromechanical oscillator networks in practice [12–18].

Synchronization is a ubiquitous phenomenon found in coupled oscillator systems [10,19]. The heart beat is a result of the synchronized motion of pacemaker cells [20], circadian rhythm arises because of coordinated body physiology [21], and the global positioning system relies on the synchronized operation of clocks. On the nanoscale, synchronization has been experimentally demonstrated in nanomechanical systems coupled through mechanical connections [3], electrical capacitors [9], off-chip connections [6], and an optical cavity [7,8]. However, these demonstrations were limited to only two oscillators. Achieving synchronization in large micromechanical oscillator networks requires scalable oscillator units and efficient and controllable coupling mechanisms [12,13,22].

Here, we experimentally demonstrate that arrays of free running micromechanical oscillators can be synchronized when coupled purely through a common electromagnetic field as predicted by theories [12,13]. A conceptual view of an array of mechanical resonators coupled through light is illustrated in Fig. 1(a). Each optomechanical oscillator (OMO) possesses a slightly different frequency of mechanical oscillation Ω_i, and is only connected through a common optical field (blue background). When a continuous wave laser is coupled to a common electromagnetic

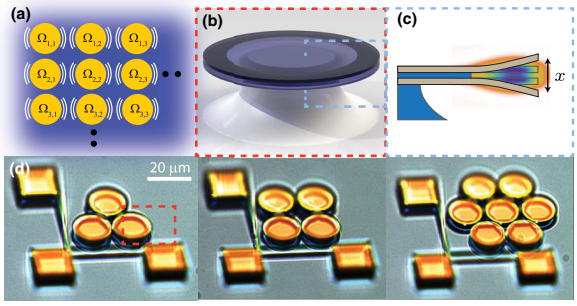

FIG. 1 (color online). Concept and devices. (a) Concept of mediating coupling between mechanical oscillators (yellow) through a global optical field (blue). The optical field provides energy for each mechanical oscillator to vibrate at their natural frequencies $\Omega_{i,j}$ and also provide coupling between each mechanical oscillator forming an all-to-all coupling topology. When the optical coupling is strong, the oscillators synchronize and vibrate at a common frequency. (b) A schematic of each individual double disk. The edges are partly suspended to allow for mechanical vibration. (c) Cross section of a double disk showing the mechanical and the optical mode shapes. (d) Optical microscope images of coupled optomechanical double-disk oscillator arrays. The oscillators are mechanically separated by a narrow gap (~150 nm) and coupled solely through the optical evanescent field. The squares and strings are support structures for tapered optical fibers.

field mode spanning several micromechanical oscillators, the light can provide both the drive for self-sustaining oscillations and the necessary coupling between the individual oscillators for synchronization through optical forces. When the laser power is just above the self-sustaining oscillation threshold of the mechanical oscillators, they are expected to vibrate at their natural frequencies Ω_i. When the laser power is high so that the optically mediated coupling is strong enough to overcome the difference in Ω_i, the mechanical oscillators can reach synchronization.

The effective coupling between the mechanical resonators can be visualized through the following equation

$$\ddot{x}_i + \Gamma_i \dot{x}_i + \Omega_i^2 x_i = F_{\text{opt}}^{(i)},$$
$$F_{\text{opt}}^{(i)} \propto |b(x_i, \ldots, x_j)|^2, \quad (1)$$

where x_i, Γ_i, and Ω_i are the mechanical displacement, damping, and mechanical frequency of the ith OMO and $b(x_i, \ldots, x_j)$ is the amplitude of the coupled optical supermode that spatially spans all cavities in the array. It is clear from the equation above that the optical force F_{opt} depends on the energy stored in the optical supermode, which is affected by the displacement of each individual cavity. Therefore, the optical field provides an effective nonlinear mechanical coupling between the different oscillators that form the basis for synchronization [7,8,13]. The onset of synchronization, which intrinsically relies on nonlinearity [23], could therefore be captured as F_{opt} is increased through increasing the optical driving power [7].

The individual oscillator we use is a double-disk OMO [Figs. 1(b) and 1(c)] composed of two free-standing silicon nitride circular edges that support high quality (Q) factor optical and mechanical modes [24,25]. The colocalized modes shown in Fig. 1(c) lead to a strong coupling between the optical and the mechanical degree of freedom. When the cavity is excited by a continuous wave laser above the oscillation threshold, the free-standing edges oscillate coherently and modulate the laser producing a radio frequency (rf) tone at the mechanical frequency of the vibrating edges. Fabrication variation causes the mechanical frequency of different OMOs in our arrays to spread around ± 1 MHz centered at 132.5 MHz [26].

We fabricate micromechanical oscillator arrays with double-disk OMOs that are optically coupled through the evanescent field. The OMOs are physically separated by a narrow gap ($\sim$150 nm), which precludes any mechanical connections while the optical evanescent field can still propagate through the gap. Mechanical coupling through the substrate connection is negligible as the mechanical mode we excite is a high Q mode that is well isolated from the substrate [24].

We excite the optical supermode that spatially spans over all cavities to ensure that there is optical coupling among all

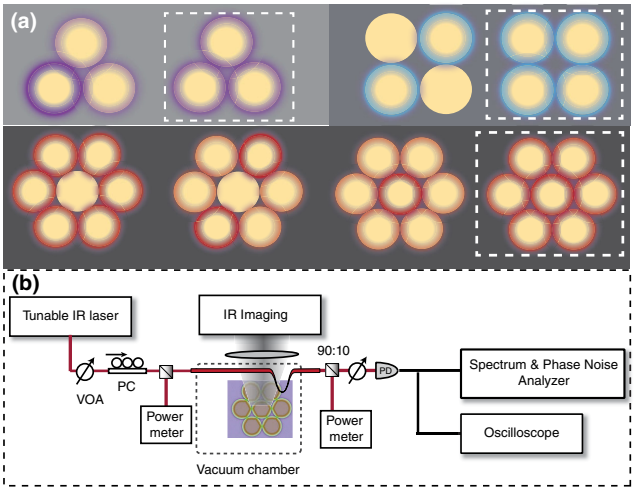

FIG. 2 (color online). Experimental configuration. (a) Optical supermode spatial structures. The colored halos show where the optical cavity field resides for different types of arrays. The more opaque colors illustrate higher cavity field intensities when compared to the rest of the cavities. The supermodes that spatially span over all cavities with equal intensities are identified by dashed lines. (b) Experimental setup. The coupled optomechanical oscillator array is placed in a vacuum chamber and excited by a tunable infrared (IR) camera through a tapered optical fiber. The optical power and polarization are controlled by an variable optical attenuator (VOA) and a fiber polarization controller (PC). The optical transmission is detected by an amplified photodiode (PD) and analyzed by an oscilloscope and a spectrum analyzer.

cavities [Fig. 2(a), dashed boxes]. The strong optical coupling between the optical modes of each individual cavity a_i leads to the formation of optical supermodes b_m that have different optical frequencies and spatial geometries [26]. Figure 2(a) illustrates the spatial intensity profile of different optical supermodes b_m when the optical resonant frequency of the individual cavity ω_i is identical. The higher intensity regions are illustrated by higher opacity of the halos around the cavities. We position a tapered optical fiber to the close proximity of one OMO in the arrays to couple light to the spatial evenly distributed optical modes [dashed lines in Fig. 2(a)] while using an infrared (IR) camera to monitor the scattered intensity from the arrays, making sure all OMOs are excited. We monitor the transmission through the tapered fiber by an amplified photodiode and feed the electrical signal to a spectrum analyzer.

We show the onset of synchronization by increasing the excitation laser power, which effectively increases the coupling between the OMOs. The laser wavelength is blue detuned relative to the resonance of the optical supermode that evenly spans all the OMOs [Fig. 2(a), dashed boxes], enabling optomechanical amplification. In the three coupled OMO array, as the laser power increases well beyond the oscillation threshold for each individual oscillator, the rf spectrum of the OMOs shows many strong

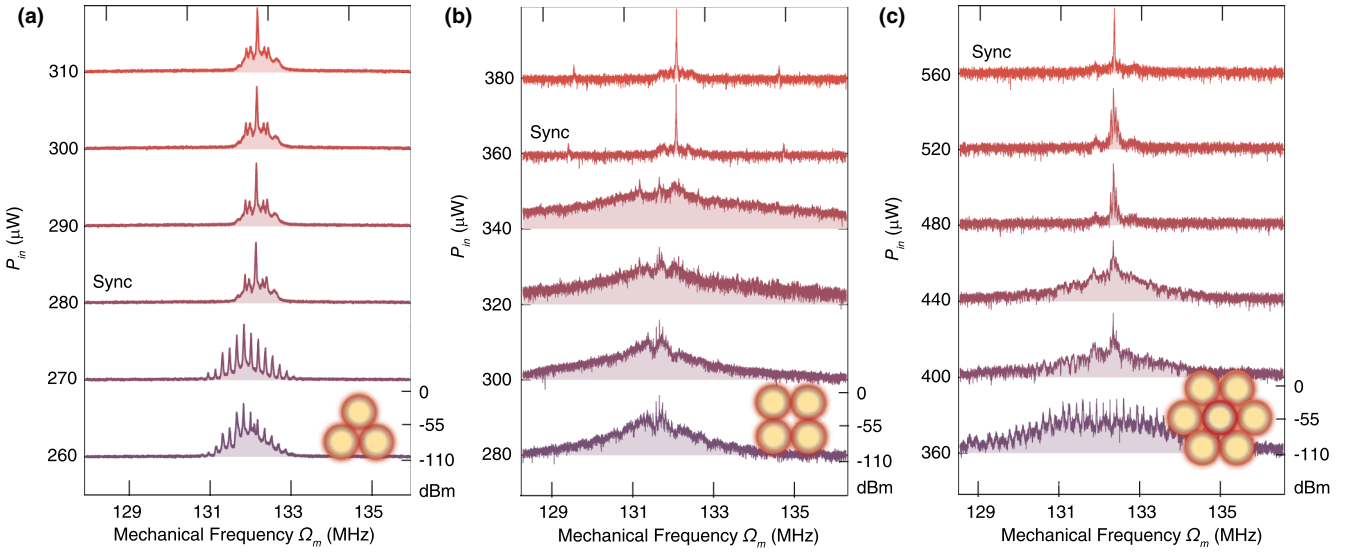

FIG. 3 (color online). Synchronization in arrays of OMOs. Optical power spectrum of the (a) three-, (b) four-, and (c) seven-OMO system as the input optical power increases. The vertical scale is from −110 to 0 dBm for each trace. Synchronization is characterized by the sudden noise floor drop and the emergence of a single frequency in the optical power spectrum as indicated in the graphs. The disorder in natural mechanical frequencies and incoherent dynamics before the onset of synchronization is evident from the rf peaks and the broad noise floor. The seven-resonator array (c) shows multiple changes of noise shapes before eventually synchronizing, indicating the presence of multiple oscillation states as a result of many OMOs.

oscillation peaks and a broad noise floor [Fig. 3(a)]. The distinct oscillation peaks form because Ω_i is different for each OMO and they beat to generate many rf tones [30,31]. The increase in the noise floor is likely due to the finite interaction between the mechanical modes mediated by the optical field but not yet strong enough to transition into a locked state [7,32,33]. As the laser power further increases to $P_{\text{in}} = 280\ \mu$W, the onset of synchronization [Fig. 3(a)] is evident as the peaks on the rf spectrum merge into a single large peak and the noise floor is reduced. The much weaker sidebands around the main oscillation signal are due to the much weaker oscillatory motion induced by thermal force displacing the OMOs from the synchronized state [7]. In the four and seven coupled OMO arrays, similar to the three-cavity system, we observe beating between different mechanical modes and a broad noise floor when the optical power is below the synchronization threshold. As the laser power is increased, a single oscillation peak appears accompanied by a sudden drop in the noise floor, signifying the onset of synchronization [Figs. 3(b) and 3(c)].

We show that in large arrays of OMOs, the phase noise of the synchronized signal can be reduced below the thermomechanical noise limit of an individual OMO by almost 10 dB. The phase noise of the modulated output light is expected to drop as the oscillators are synchronized [6,10,11]. We measure the phase noise of our oscillators at 10 kHz offset from the carrier oscillation frequency, where the phase noise of our oscillator is dominated by thermomechanical fluctuation [26,34–36], a fundamental limit imposed to the mechanical oscillator due to the thermal bath of the environment. In Fig. 4(a), we show the measured phase noise in a 1×2 OMO array [8]. As shown in Fig. 4(a), the single OMO phase noise [26] at low optical power is ~ -60 dBc/Hz and gradually increases as the laser power is increased. The increase of phase noise is due to phase slipping between the two OMOs [6]. As the coupling between the OMOs increases with increasing laser power, they synchronize. As expected, we observe the phase noise drops by ∼3 dB as the two OMOs move from the one-OMO oscillating state to a synchronized oscillation state. Since the oscillators are nearly identical, synchronized oscillations can be viewed as two oscillators operating coherently, providing a larger effective mass while not reducing the oscillation frequency [35]. In Fig. 4(c), we show the measured phase noise of each large array of oscillators by driving the system at high optical powers at the optimal optical detuning where the phase noise is a minimum [26]. The lowest phase noise measured in each array of different size is plotted in Fig. 4(b). The measured phase noise follows the $1/N$ dependence predicted by theory [10,11,35,37].

The drop in phase noise can also be used to determine the number of synchronized OMOs in a single array oscillating in different states. We measure the phase noise in the 2×2 array as the oscillators change from a state where only two OMOs are oscillating to a state where all four OMOs are oscillating, as we infer from the light scattering intensities captured on the IR camera. Figure 4(c) shows the power spectrum of the transmitted light when the laser is tuned

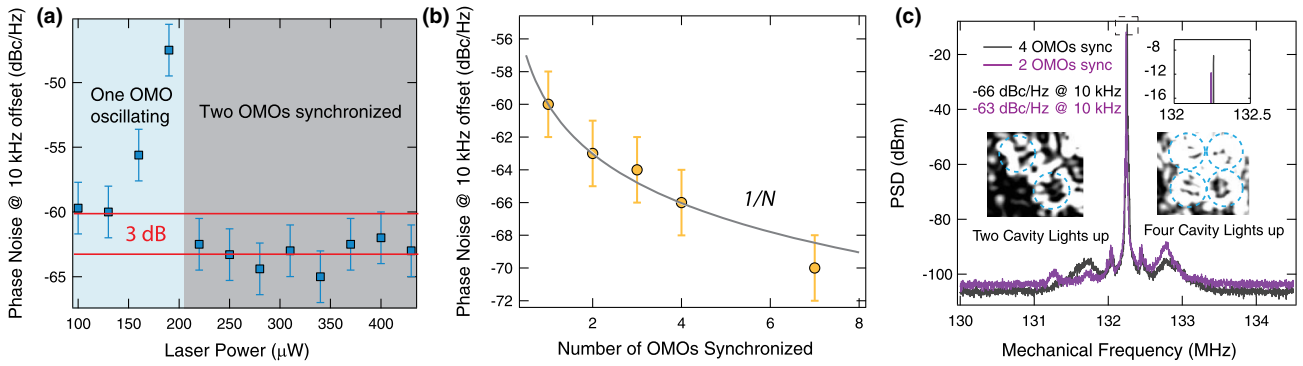

FIG. 4 (color online). Phase noise in synchronized arrays. (a) Phase noise in a two-OMO system at a 10 kHz carrier offset as the laser power is increased. The noise increases due to mode competition between possible oscillation states and then decreases by ∼3 dB below the noise level of the one-OMO oscillation state. (b) The phase noise of the synchronized oscillation signal for different sizes of OMO arrays. The gray curve is the phase noise level predicted by theory for near-identical synchronized oscillators. (c) Power spectrum of a state where four OMOs are oscillating (black) and of a state where two OMOs are oscillating (purple). The phase noise drops by ∼3 dB following the transition. The inset shows an enlargement near the peak and captured IR images for the two- and four-OMO synchronized state, respectively.

from an optical mode that spans two cavities to an optical mode that spans all four cavities [Fig. 2(a)] while staying at the same optical power. Following the transition, the four-OMO oscillation state shows an increase of ∼3 dB in the oscillation signal and a ∼3 dB drop in the phase noise. At the same time, all four resonators light up on the IR camera. The drop in phase noise and the change of scattering intensity on the IR camera strongly indicate that the array changes from two to four synchronized oscillators.

In conclusion, we demonstrate synchronization in integrated arrays of micromechanical oscillators coupled through a common optical field. We show the onset of synchronization in the arrays by tracking the emergence of a single oscillation frequency in the optical power spectrum. Synchronization is further corroborated by the drop in phase noise in the oscillator arrays. The reduction of phase noise with oscillator array size and the scalability of our devices could enable low noise and high power integrated frequency sources. Our work paves a path towards large scale monolithically fabricated oscillator networks that have the potential to compete with the performance of bulk resonators and to exhibit rich nonlinear dynamics, opening the door to novel metrology, communication, and computing techniques [38,39].

We acknowledge Richard Rand and Gustavo Wiederhecker for a fruitful discussion about our results. The authors gratefully acknowledge support from DARPA though Grant No. W911NF-11-1-0202. The authors also acknowledge Applied Optronics and DARPA for Grant No. W911NF-14-C0113. This work was performed in part at the Cornell NanoScale Facility, a member of the National Nanotechnology Infrastructure Network, which is supported by the National Science Foundation (Grant No. ECCS-0335765). This work made use of the Cornell Center for Materials Research Facilities supported by the National Science Foundation under Grant No. DMR-1120296. The authors also acknowledge Paul McEuen for use of lab facilities.

*Corresponding author.
ml292@cornell.edu

[1] H. G. Craighead, Science **290**, 1532 (2000).
[2] J. Zhang, H. P. Lang, F. Huber, A. Bietsch, W. Grange, U. Certa, R. Mckendry, H.-J. Gntherodt, M. Hegner, and Ch. Gerber, Nat. Nanotechnol. **1**, 214 (2006).
[3] S.-B. Shim, M. Imboden, and P. Mohanty, Science **316**, 95 (2007).
[4] I. Bargatin, E. B. Myers, J. S. Aldridge, C. Marcoux, P. Brianceau, L. Duraffourg, E. Colinet, S. Hentz, P. Andreucci, and M. L. Roukes, Nano Lett. **12**, 1269 (2012).
[5] C. T.-C. Nguyen, IEEE Trans. Ultrasonics, Ferroelectrics, and Frequency Control **54**, 251 (2007).
[6] M. H. Matheny, M. Grau, L. G. Villanueva, R. B. Karabalin, M. C. Cross, and M. L. Roukes, Phys. Rev. Lett. **112**, 014101 (2014).
[7] M. Bagheri, M. Poot, L. Fan, F. Marquardt, and H. X. Tang, Phys. Rev. Lett. **111**, 213902 (2013).
[8] M. Zhang, G. S. Wiederhecker, S. Manipatruni, A. Barnard, P. McEuen, and M. Lipson, Phys. Rev. Lett. **109**, 233906 (2012).
[9] D. K. Agrawal, J. Woodhouse, and A. A. Seshia, Phys. Rev. Lett. **111**, 084101 (2013).
[10] A. Pikovsky, M. Rosenblum, and J. Kurths, *Synchronization: A Universal Concept in Nonlinear Sciences* (Cambridge University Press, Cambridge, England, 2003).
[11] H.-C. Chang, X. Cao, U. K. Mishra, and R. York, IEEE Trans. Microwave Theory Tech. **45**, 604 (1997).
[12] G. Heinrich, M. Ludwig, J. Qian, B. Kubala, and F. Marquardt, Phys. Rev. Lett. **107**, 043603 (2011).
[13] C. A. Holmes, C. P. Meaney, and G. J. Milburn, Phys. Rev. E **85**, 066203 (2012).

[14] S. Y. Shah, M. Zhang, R. Rand, and M. Lipson, Phys. Rev. Lett. **114**, 113602 (2015).
[15] A. H. Safavi-Naeini, J. T. Hill, S. Meenehan, J. Chan, S. Grblacher, and O. Painter, Phys. Rev. Lett. **112**, 153603 (2014).
[16] M. Aspelmeyer, T. J. Kippenberg, and F. Marquardt, Rev. Mod. Phys. **86**, 1391 (2014).
[17] T. Botter, D. W. C. Brooks, S. Schreppler, N. Brahms, and D. M. Stamper-Kurn, Phys. Rev. Lett. **110**, 153001 (2013).
[18] A. B. Shkarin, N. E. Flowers-Jacobs, S. W. Hoch, A. D. Kashkanova, C. Deutsch, J. Reichel, and J. G. E. Harris, Phys. Rev. Lett. **112**, 013602 (2014).
[19] S. Strogatz, *Sync: The Emerging Science of Spontaneous Order* (Hyperion, New York, NY, 2003).
[20] C. S. Peskin, *Mathematical Aspects of Heart Physiology* (Courant Institute of Mathematical Sciences, New York University, 1975).
[21] S. M. Reppert and D. R. Weaver, Nature (London) **418**, 935 (2002).
[22] R. Lauter, C. Brendel, S. J. M. Habraken, and F. Marquardt, arXiv:1501.01509.
[23] M. C. Cross, A. Zumdieck, R. Lifshitz, and J. L. Rogers, Phys. Rev. Lett. **93**, 224101 (2004).
[24] M. Zhang, G. Luiz, S. Shah, G. Wiederhecker, and M. Lipson, Appl. Phys. Lett. **105**, 051904 (2014).
[25] Q. Lin, J. Rosenberg, X. Jiang, K. J. Vahala, and O. Painter, Phys. Rev. Lett. **103**, 103601 (2009).
[26] See Supplemental Material at http://link.aps.org/supplemental/10.1103/PhysRevLett.115.163902 for additional data and theoretical analysis, which includes Refs. [27–29].
[27] H. A. Haus, *Waves and Fields in Optoelectronics* (Prentice-Hall, Englewood Cliffs, NJ, 1984).
[28] D. Leeson, Proc. IEEE **54**, 329 (1966).
[29] T. Laurila, T. Joutsenoja, R. Hernberg, and M. Kuittinen, Appl. Opt. **41**, 5632 (2002).
[30] M. Hossein-Zadeh and K. J. Vahala, Appl. Phys. Lett. **93**, 191115 (2008).
[31] C. Huang, J. Fan, R. Zhang, and L. Zhu, Appl. Phys. Lett. **101**, 231112 (2012).
[32] Y. Okawachi, K. Saha, J. S. Levy, Y. H. Wen, M. Lipson, and A. L. Gaeta, Opt. Lett. **36**, 3398 (2011).
[33] P. DelHaye, K. Beha, S. B. Papp, and S. A. Diddams, Phys. Rev. Lett. **112**, 043905 (2014).
[34] K. Y. Fong, M. Poot, X. Han, and H. X. Tang, Phys. Rev. A **90**, 023825 (2014).
[35] S. Tallur, S. Sridaran, S. Bhave, and T. Carmon, in *Frequency Control Symposium (FCS), 2010 IEEE International*, (IEEE, New York, 2010), pp. 268–272.
[36] M. Hossein-Zadeh, H. Rokhsari, A. Hajimiri, and K. J. Vahala, Phys. Rev. A **74**, 023813 (2006).
[37] M. C. Cross, Phys. Rev. E **85**, 046214 (2012).
[38] F. Hoppensteadt and E. Izhikevich, IEEE Trans. Circuits Syst. I **48**, 133 (2001).
[39] A. Mari, A. Farace, N. Didier, V. Giovannetti, and R. Fazio, Phys. Rev. Lett. **111**, 103605 (2013).